Effect of Fiber Hybridization on Basic Mechanical Properties of Concrete

by Stamatina G. Chasioti and Frank J. Vecchio

In recognition of the gradual and multi-scale process of cracking, this paper investigates the beneficial effects of fiber hybridization on the basic mechanical properties of concrete. Allowing for these benefits in the mechanical performance may potentially lead to reduced production and construction costs. An experimental investigation was undertaken involving normal-strength concrete in which two types of steel fibers were used: high-strength straight steel microfibers with a length of 13 mm (0.51 in.), and hooked-end macrofibers with a length of 30 mm (1.18 in.). Comparisons between hybrid steel fiber-reinforced concrete (HySFRC) specimens and monofiber counterparts with the same total volumetric ratio highlight its superior performance. Synergy in compression is identified by an enhanced confinement mechanism, in tension by improved post-cracking resistance at both low and high crack openings, and in bending through enhanced fracture toughness. Additionally, a variant of the dogbone-type specimen for tests in direct tension was developed. The novel configuration is more suitable for concrete containing fibers and it is easy to construct and test.

Keywords: direct tension; dog-bone specimen; four-point bending; hybrid steel fiber-reinforced concrete; synergy.

INTRODUCTION

Fibers are added to concrete to compensate for its brittle and weak nature in tension; resulting materials are commonly referred to as high-performance fiber-reinforced cementitious composites (HPFRCCs). Their constitutive characteristics in tension may involve increased strength and toughness, higher ductility, enhanced matrix stiffness, or hardening in the post-cracking response relative to regular concrete.[1,2] Most HPFRCCs used today contain a single type of fiber that usually contributes to the attainment of one of the characteristics aforementioned.[1,3] Hybridization is the technique of maximizing and combining the benefits of fiber addition in an effective way.

Mixture design optimization based on effective fiber combination is premised on the assumption that the manner in which the fibers act is influenced by the concrete microstructure. Because one type of fiber is only effective for a limited range of strain or crack opening, multiple fiber types may be used to achieve the desired properties over a wider range of deformation. It is generally thought that capturing the coalescence of microcracks and bridging the opening of the macrocracks leads to increased energy absorption. Over recent years, many combinations have been tested aiming to address these two levels of crack growth; they are generally summarized under two main categories, listed as follows.[3-5]

Hybrids based on the fiber constitutive response: The main variable herein is the fiber stiffness. Fibers with high moduli of elasticity (made from steel or kevlar) are considered to effectively bridge microcracks, while ones with low moduli (polypropylene) are mobilized at larger crack openings.

Hybrids based on fiber dimensions and anchorage mechanism: The fibers under this category are termed microfibers and macrofibers.[6] The first have been proven to arrest the coalescence of cracks at an early stage, conditionally leading to strength increase, while the latter help increase the post-cracking toughness. Their effectiveness depends on the anchorage mechanism.

There is, however, an emerging third category: **hybrids based on fiber function**. That is, one type of fiber that improves the fresh or early-age properties, such as workability and shrinkage, typically made out of polypropylene, and a second type, usually steel, for the improvement of the mechanical properties.[7]

Nevertheless, studies seem to contradict each other on the findings regarding the range and the magnitude of the effectiveness of each fiber based on the aforementioned criteria. For example, ultra-high-performance fiber-reinforced Concrete (UHPFRC) shows strain hardening behavior in tension using steel fibers in the range of 0.1 to 0.3 mm (0.004 to 0.012 in.) diameter and 6 to 20 mm (0.24 to 0.79 in.) length.[8] On the other hand, Chasioti and Vecchio[9] tested direct tension specimens using the same fibers in the context of normal-strength concrete (NSC); the results showed strain softening after the matrix had cracked, with the main effect being on the initial stiffness of the matrix. Plizzari et al.[10] tested beams with the same steel fiber using NSC and high-strength concrete (HSC). The result was that the fibers were more effective in HSC and resulted in smaller crack widths. The first case highlights the influence of the matrix and the second, the influence of the bond in the response of the fiber-reinforced concrete (FRC).

Concrete matrix characteristic strength is, in fact, an influential parameter for the response of FRC. Studies on the pullout mechanisms of fibers have proven the significance of the matrix composition and microstructure on the bond strength of the fibers and, therefore, on the behavior of the composite. Markovic et al,[11] Banthia,[12] and Lawler et al.[7] are among many researchers identifying the influence of the type and the cement volumetric content, the granular composition and the sand content, the admixtures substituting cement such as silica fume, and the maximum size of the aggregate. The parameters aforementioned, in conjunction with the fiber geometry, quantity, and material, not only influence
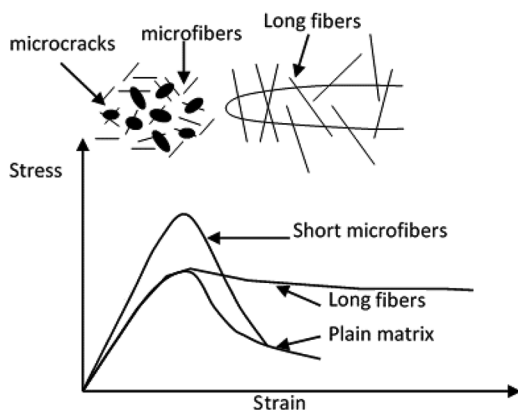
Fig. 1—Illustration of different sizes of fibers on crack bridging (adopted from Betterman et al.[12]).

Table 1—Fiber properties and geometry

Fiber	l_f, mm (in.)	d_f, mm (in.)	AR_f	f_{uf}, MPa (ksi)	E_f, MPa (ksi)
RC80/30BP	30 (1-3/16)	0.38 (0.015)	79	3070 (445.2)	200,000 (29,000)
OL13/.20	13 (33/64)	0.21 (0.008)	62	2750 (398.8)	200,000 (29,000)

the magnitude but also the strain range of the fiber contribution. As a result, the FRC response is mainly governed by the tripartite interaction between matrix, fiber, and bond. Figure 1[13] shows the influence of fibers of different size to the crack bridging and the FRC response compared to the plain concrete. The distinction between "short" and "long" fibers is therefore a significantly relative quantity.

Hybrid fiber-reinforced concrete (HyFRC) attempts to take advantage of the different fiber contributions by combining them. In well-designed hybrid composites, the response is not simply the addition of separate fiber contributions; rather, there is a positive interaction that provides the new composite with improved characteristics. Hybridization is essentially an optimization process and the positive interaction between the fibers is often termed as "synergy." Several efforts have been made by researchers to identify synergy through the optimization of the relative fiber ratio,[14,15] optimal fiber material and geometry in flexure,[16] and in direct tension.[17] However, in some cases, no synergy was identified, and when it was, the effect was influenced by the matrix. In fact, for some mixtures, synergy may be seen only under particular loading conditions such as in direct shear.[18]

Work presented herein is part of a larger study whose purpose is to examine the so-called synergy between fibers, both at the material and structural levels, in terms of strength, displacement capacity, and failure mode. The benefits of fiber hybridization on the shear behavior and cracking properties of HySFRC containing conventional steel reinforcement were evaluated by Chasioti and Vecchio.[19] Hence, the main focus of this paper is the mechanical response in regards to compression, direct tension, and bending of HySFRC. Hooked-end steel macrofibers and straight, short microfibers are added into a NSC matrix containing coarse aggregates. Concrete batches reported herein are the same as in Chasioti and Vecchio[19] for the same specimen notation. Comparisons against monofiber mixtures with the same *total* amount of fibers were performed; hence, potential benefits in the materials response would be directly related to cost reduction.

Compression tests were performed using cylinders for assessing the effects of hybridization on the axial stress-strain curve, and also on cubes for correlation of the compressive strength. Unnotched simply supported beams were tested under four-point loading to assess the flexural response. For

the direct tension behavior, a new "dog-bone type" specimen was designed, constructed, and used. This new tension specimen configuration is suitable for concrete containing fibers, being easy to construct and test and overcoming some of the deficiencies of other tension specimens that have been used.

RESEARCH SIGNIFICANCE

The merits of hybridization rely on the fact that cracking is a gradual multi-scale process. Optimization of the fiber combination so that fracture is restrained on multiple levels leads to concrete with enhanced mechanical characteristics. This paper examines synergies in the mechanical properties of hybrid mixtures compared to those of monofiber counterparts with the same total fiber volumetric ratio. Allowing for these benefits in the mechanical performance may potentially lead to reduced production and construction costs.

EXPERIMENTAL INVESTIGATION

The main objective of this study is to examine the so-called synergy between diverse fibers in terms of strength, fracture toughness, and displacement capacity in the context of NSC containing aggregates. This goal is evaluated at multiple levels. The experimental program, involving tests in tension, compression, and bending, includes concrete with hybrid steel fibers in a ratio of 1:1, at several total volumetric ratios, compared against single fiber counterparts with the same total amount of fibers. In total, eight different concrete mixtures were cast, containing a total of 0.75%, 1%, 1.5%, and 2% fibers per unit weight of concrete. The specimen notation is as follows. First index: <u>Hy</u> for hybrid fibers in a ratio of 1:1; <u>SL</u> for single type of fiber-long (macrofiber); <u>SS</u> for single type of fiber-short (microfiber). Second index: total V_f, equal to 0.75%, 1.0%, 1.5%, and 2.0%. Although many other types and lengths of fiber can be combined, this paper focuses on just one combination to illustrate potential benefits. Test data reported herein can be used to contribute to the broader database of concrete hybrids.

Constitutive materials

Two types of steel fibers differing in geometry (that is, length, aspect ratio and anchorage mechanism) were used. Table 1 summarizes the pertinent fiber properties and characteristics employed in this study. The RC-80/30-BP hooked-end fibers and the straight OL13/.20 served as the macrofibers and the microfibers, respectively, in a ratio of 1:1.

The mixture design of all eight composites is shown in Table 2. GUL cement (portland cement with limestone filler), typical for construction in Canada, was used as a binder. The water-cement ratio (*w/c*) was kept constant at 0.45. Washed coarse aggregate, with a maximum grain size of 9.5 mm (3/8 in.), was graded according to the CSA

Table 2—Mixture design

Material	Hy0.75	Hy1.0	SL1.0	SS1.0	Hy1.5	SL1.5	SS1.5	Hy2.0
Cement, kg/m^3 (lb/ft^3)	432 (26.96)	432 (26.96)	432 (26.96)	432 (26.96)	432 (26.96)	432 (26.96)	432 (26.96)	432 (26.96)
Water, kg/m^3 (lb/ft^3)	194 (12.11)	194 (12.11)	194 (12.11)	194 (12.11)	194 (12.11)	194 (12.11)	194 (12.11)	194 (12.11)
Sand, kg/m^3 (lb/ft^3)	972 (60.68)	972 (60.68)	972 (60.68)	972 (60.68)	972 (60.68)	972 (60.68)	972 (60.68)	972 (60.68)
Coarse aggregate, kg/m^3 (lb/ft^3)	798 (49.82)	792 (49.44)	792 (49.44)	792 (49.44)	778 (48.57)	778 (48.57)	778 (48.57)	764 (47.69)
Total steel fibers, kg/m^3 (lb/ft^3)	59 (3.68)	78 (4.87)	78 (4.87)	78 (4.87)	117 (7.30)	117 (7.30)	117 (7.30)	156 (9.74)
HRWRA, mL (oz)	4.5 (4.5)	5 (5)	4 (4)	3.75 (3.75)	8.2 (8.2)	7.9 (7.9)	7.9 (7.9)	8.2 (8.2)
Slump, mm (in.)	135 (5-5/16)	130 (5-1/8)	140 (5-3/64)	140 (5-3/64)	170 (6-1/16)	170 (6-1/16)	160 (6-19/64)	170 (6-1/16)
γ, kN/m^3 (lb/ft^3)	23.7 (151)	23.8 (151)	23.4 (149)	23.4 (150)	23.9 (152)	24.4 (155)	23.9 (152)	24.3 (154)
γ/γ_n	0.99	0.98	0.97	0.97	0.98	1.00	0.98	0.98

Notes: γ is measured unit weight; and γ_n is nominal unit weight (calculated from composition).

A23.1-09/A23.2-09.[20] Aggregate and sand moisture content were accounted for in each batch, and the water added was appropriately adjusted. The matrix was kept the same for all composites for comparison purposes, apart from the fact that fiber content replaced an equivalent volume of coarse aggregate. The ratios of cement and fine aggregate in the mixture ensured adequate surface coating for the fibers. Fresh concrete properties were enhanced using a polycarboxylate high-range water-reducing admixture (HRWRA). Hybrid composites were more viscous due to the higher relative area of solids and, therefore, the amount of HRWRA had to be adjusted. A target slump of approximately 150 mm (6 in.) for all batches was necessary to ensure adequate concrete compaction for the specimens containing conventional steel reinforcement.[19] The degree of compaction of the specimens is quantified in Table 2 by the specific measured weight of the batch γ normalized over the nominal values γ_n for each different mixture, calculated from composition of its constituents.

Specimens

All specimens were prepared using a high-energy mixer and consolidated under external vibration. They were cured under wet burlap and plastic cover for 7 days, followed by 21 days of dry curing in ambient lab conditions, before testing. Figure 2 shows the tests specimens used in this study. Three cylinders, three cubes, two modulus of rupture beams, and three direct tension specimens were cast for each of the 11 batches; 121 specimens in total.

Uniaxial compressions tests—Cylinder tests were performed to evaluate the full compressive stress-strain response of the concrete (Fig. 2(a)). The cylinder dimensions were 100 mm (4 in.) in diameter and 200 mm (8 in.) in height. For correlation purposes, cubes (Fig. 2(b)), 150 x 150 x 150 mm (6 x 6 x 6 in.) were used to obtain the peak compressive stress $f'_{cc,150}$ as well. The tests were performed under a constant rate of 250 ± 50 kPa/s (35 ± 7 psi/s) in accordance with ASTM C469/C469M.[21]

Flexural tests—The ASTM C1609/C1609M-12[22] standard served as the reference for performance of the modulus of rupture (MOR) tests. Unnotched beams were tested under four-point bending with a constant loading rate of 0.006 mm/s (0.00024 in./s) until the attainment of the peak load; thereafter, the rate was gradually increased up to a
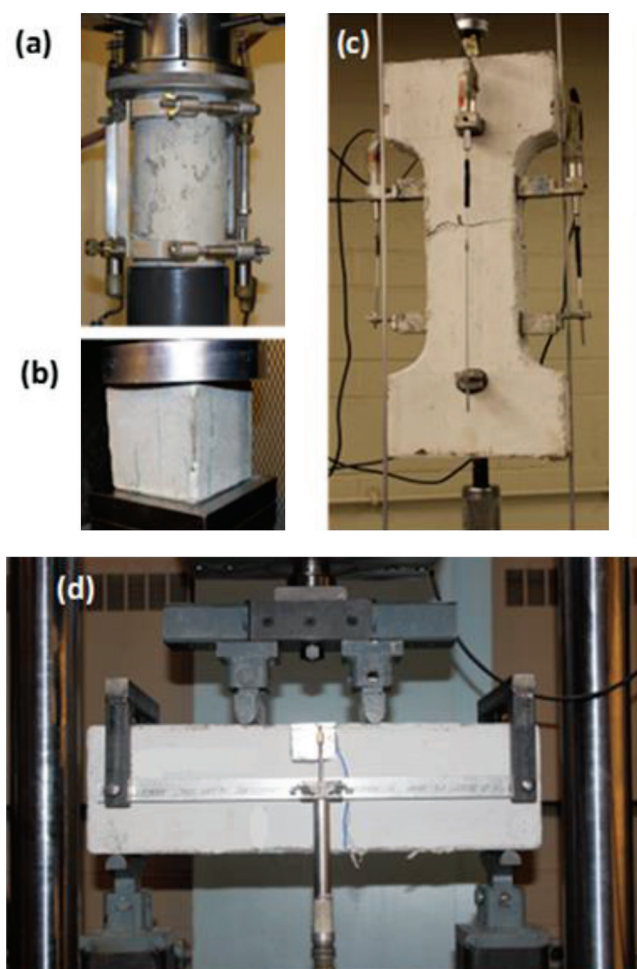

Fig. 2—Test specimens: (a) 100 x 200 mm (4 x 8 in.) cylinder; (b) 150 mm (6 in.) cube; (c) uniaxial tension specimen; and (d) modulus of rupture specimen.

maximum of 0.02 mm/s (0.0008 in./s). The cross-sectional dimensions were 152 x 152 mm (6 x 6 in.) and the total length of the specimen was 533 mm (21 in.). The beam geometry and the test setup arrangement is shown in Fig. 2(d). The clear span between the supports was 457 mm (18 in.), and two-point loads were applied symmetrically over the clear span of the specimen. Specimens were turned to their sides with respect to the casting direction when placed on the supports before testing. This was done to avoid the bias in

the test results that would be caused if the fibers were not uniformly distributed within the matrix. (In that case, fibers would gravitate and the test result would be biased based on whether the top or bottom side was in tension or in compression.) The vertical displacement of the beam was measured continuously by means of two linear variable displacement transducers (LVDTs), one on each side, along the midsection in the segment of zero shear. The test continued until at least a net midspan deflection of $L/150$ was achieved (that is, 3 mm [0.12 in.]) conforming to the ASTM C1609/C1609M-12.[22] Typically, however, the test was not terminated until the midspan deflection reached 7.5 mm (0.3 in.) to ensure adequate data acquisition for a greater range of midspan deflection in the post-peak region.

Configuration of direct tension specimen

Flexural specimens are relatively simple to construct and test, and provide typically minimal discrepancy in the results. The test is well established in the guidelines as an indirect measure of the tensile performance of concrete in the absence of a better and more reliable specimen. The material tensile strength is then found from the applied load by calculation based on the assumption of linear elastic behavior. This method of inverse analysis works well for regular concrete, but uncertainties associated with the performance of FRC in tension suggest the need for a more direct and reliable test setup. In 2006, Naaman and Reinhardt[23] proposed a benchmark for the classification of high-performance composites, calling for the development of a rational tensile test. The motivation is based on the recognition that either strain-softening or strain-hardening composites can result in deflection hardening in bending, obfuscating the tensile strength. To address these issues, direct tension tests were performed additionally to the flexural tests, and a reliable test specimen is proposed herein.

Direct tension tests—The test specimen used is shown in Fig. 2(c). The dog-bone-shaped specimen was mounted in a 245 kN (55 kip) MTS machine through two 19 mm (3/4 in.) threaded rods. The fact that the force is applied through threaded steel rods mounted in the test machine facilitates testing of the specimen in a greater number of laboratories that are able to test steel coupons, without purchasing of any additional special gripping equipment. The longitudinal strain was measured through four LVDTs, one on each side of the specimen. The test was performed in a displacement control mode using two external LVDTs not attached to the specimen, with a constant rate of 0.001 mm/s (0.00004 in./s) up to the attainment of peak load, and then gradually increased up to a maximum of 0.01 mm/s (0.0004 in./s).

The gripping arrangement is an important consideration in the tension test. Benson and Karihaloo,[24] Wille et al.,[25] and many other researchers reported the influence of fixed ends versus rotating ends. The use of rotating grips results in a lower-bound strength and fracture energy because failure is able to occur in the weakest area in the specimen.[24] The reason is that there is no bending moment counteracting the inherent rotation of the specimen due to the random orientation of the fibers. Hence, rotating ends were used for the direct tension test.
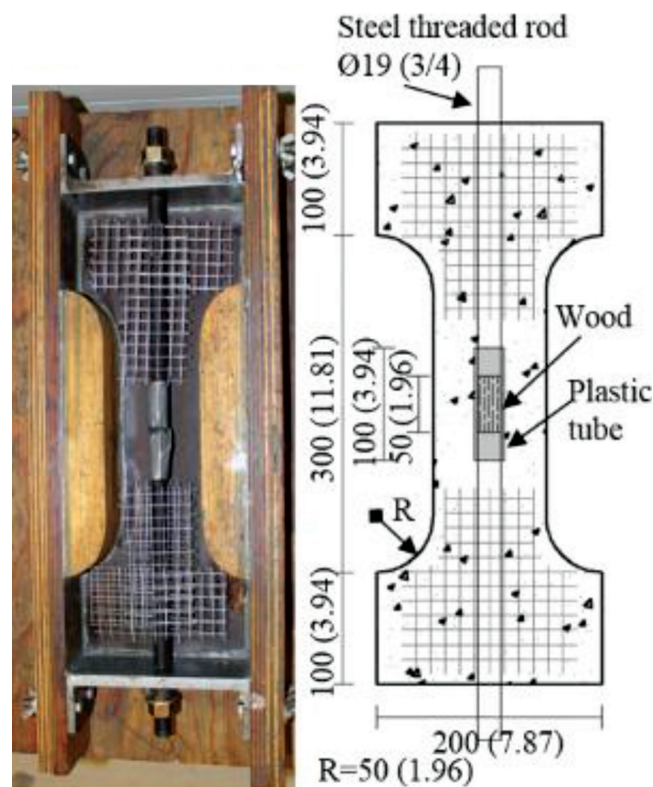

Fig. 3—Direct tension specimen; thickness equal to 70 mm (2.76 in.); dimensions in mm (in.).

The direct tension test is a sensitive and difficult test to perform.[26] Problems reported in the literature include: bond failure due to stress concentrations whereby the concrete layer close to the glued end of the specimen fails[27]; failure in the nonprismatic end regions of the specimen[27]; and bending issues, which are difficult to avoid.[24]

Specimen development—A new dog-bone-type configuration that potentially overcomes these difficulties is shown in Fig. 3. The specimen used in this study was based on the well-known dog-bone-shaped specimen. The external dimensions were kept the same for ease of construction. The total length of the specimen was 500 mm (19.69 in.) with a thickness of 70 mm (2.76 in.), more than two times greater than the longest fiber to ensure random fiber orientation. Threaded steel rods at the top and the bottom of the specimen were embedded for a length of 225 mm (8.86 in.) on each side. In the middle of the specimen, continuing in the line of the steel end rods, was a wooden rod with the same diameter and a length of 50 mm (1.97 in.). The wood was used only for the alignment of the two end rods and offered no resistance in tension. In this manner, bending induced by the specimen itself was minimized, although inherent bending due to the fiber orientation and the heterogeneity of the material could not be excluded. Further, to ensure that failure occurred in the prismatic part of the specimen where shape effects are absent, end regions were strengthened so that stresses propagated smoothly through the bonded length of the threaded rod until they reached the mid-part. The end regions were reinforced by two layers of steel wire mesh with a 12.7 mm (0.5 in.) grid to avoid splitting effects due to the small concrete cover. In the middle part of the

Table 3—Compression test results

	Hy0.75	Hy1.0		SL1.0	SS1.0	Hy1.5			SL1.5	SS1.5	Hy2.0
Batch No.		1	2			1	2	3			
Compressive tests on cubes											
$f_{cc,150}$, MPa (ksi)	63.04 (9.14)	*	*	59.29 (8.60)	61.49 (8.92)	58.40 (8.47)	61.93 (8.98)	66.74 (9.68)	59.62 (8.65)	60.27 (8.74)	55.323 (8.02)
CoV, %	2.8	*	*	2.1	1.4	0.4	1.5	1.1	0.9	1.4	0.9
Compressive tests on cylinders											
$f_{ck,100}$, MPa (ksi)	60.97 (8.84)	51.34 (7.45)	63.49 (9.21)	57.53 (9.21)	54.12 (7.85)	41.56 (6.03)	55.48 (8.05)	71.69 (10.40)	61.13 (8.87)	50.46 (7.32)	58.16 (8.44)
CoV, %	3.6	6.8	1.8	4.1	4.8	7.0	4.8	1.1	3.2	2.7	*
Mean $f_{ck,100}$, MPa (ksi)	60.97 (8.84)	57.41 (8.33)		57.53 (9.21)	54.12 (7.85)	63.59 (9.22)			61.13 (8.87)	50.46 (7.32)	58.16 (8.44)
ε_c', × 10^{-3}	2.88	2.44	3.62	2.63	1.66	*	2.26	4.07	11.27	2.15	8.29
CoV, %	4.0	20.6	11.9	23.6	14.1	*	27.7	5.6	12.0	8.7	*
E_{cs}, GPa (ksi)	37.1 (5385)	37.6 (5466)	40.67 (5899)	38.0 (5515)	50.4 (7312)	*	38.1 (5528)	33.7 (4896)	32.3 (4698)	42.1 (6109)	30.1 (4371)
CoV, %	8.43	8.86	8.91	14.08	16.02	*	17.90	1.29	11.86	16.49	*
Mean E_{cs}, GPa (ksi)	37.1 (5385)	39.1 (5683)		38.0 (5515)	50.4 (7312)	35.9 (5212)			32.3 (4698)	42.1 (6109)	30.1 (4371)
$f_{ck,100}$ / $f_{cc,150}$	0.97	*	*	0.97	0.88	0.71	0.90	1.07	1.03	0.84	1.05

*Values not measured.

dog-bone, the piece of wood and part of the threaded rods are covered by a smooth plastic tube. Thus, the stresses propagate through the rod and, along the unbonded length, the tensile force is carried by the concrete alone. The length of the plastic tube was 100 mm (3.94 in.) to provide sufficient space for the failure to occur along the weakest section or, alternatively, allow for multiple cracking. Therefore, the specimen was suitable for both tension-softening and tension-hardening materials.

EXPERIMENTAL RESULTS AND DISCUSSION
Response in compression

Table 3 summarizes the results for the cubes and cylinders tested under compression. For the cubes, only the peak compressive stress $f_{cc,150}$ was measured, while for the cylinders the peak stress $f_{ck,100}$, the strain at the peak stress ε_c', and the secant modulus of elasticity, E_{cs}, at 40% of the $f_{ck,100}$, are reported. The specimens that contained short fibers only, denoted by the SS prefix, appear slightly stiffer compared to the other two batches with the same total amount of fibers. This is likely due to increased restraint effect in the microcracking phase in the lateral direction, related to the Poisson's effect. Nevertheless, the behavior is followed by a steep post-peak, as shown in Fig. 4(a) and 4(b), because short fibers are not effective at larger strains. On the other hand, the hybrid specimens combine both the increased initial modulus of elasticity of the short fibers, with a slower rate of stiffness loss in the pre-peak response, and the increased strength capacity in the post-peak phase. Strength degradation is more gradual due to the presence of the longer fibers, for fiber ratios of both 1.0% and 1.5%, as shown in Fig. 4(a) and 4(b). Enhanced initial stiffness and a slower rate of stiffness loss in the prepeak response with respect

to the SL specimens due to the presence of short fibers in the hybrid mixture, and enhancements in the post-peak response relative to the SS specimens due to the presence of the long fibers, highlight the confinement effect present in the hybrid specimens. According to Pantazopoulou and Zanganeh,[28] the presence of short microfibers reduces the rate of dilation relative to plain concrete, particularly near the point of reversal into the range of volumetric expansion, hence increasing the energy input that would be required to disjoin the interparticle attractions that hold the material in a solid state.[29] This became evident by both measurements of the axial and volumetric strain on cylinders,[29] and it was also observed in the tests herein, in light of the fact that hybrid mixtures contained only half of the short and half of the long fibers that they were compared against. Overall, divergence of the strain at the peak stress of the ε_c' equal to 2.0 millistrain, typical for plain concrete, highlights the influence of fibers in the compressive behavior of FRC. Fibers of different lengths restraining the lateral expansion of concrete strongly resemble passive confinement effects.[28,30] As a result, the displacement capacity increases and failure becomes more ductile. Increasing fiber ratio for the HySFRC makes the confining effect more pronounced; hence, ε_c' increases, as seen in Fig. 4(c), for ratios varying from 0.75% to 2.0%. The influence of fiber hybridization and fiber ratio on the peak compressive strength is small, consistent with the present literature.

Figure 5 relates the peak compressive strengths obtained from cylinders with a diameter of 100 mm (4 in.) and a length of 200 mm (8 in.) to the strengths obtained from 150 mm (6 in.) cubes. The correlation factor calculated accordingly had a mean value of 0.93 with a coefficient of variation of 12%. The strengths of the cylinders were greater
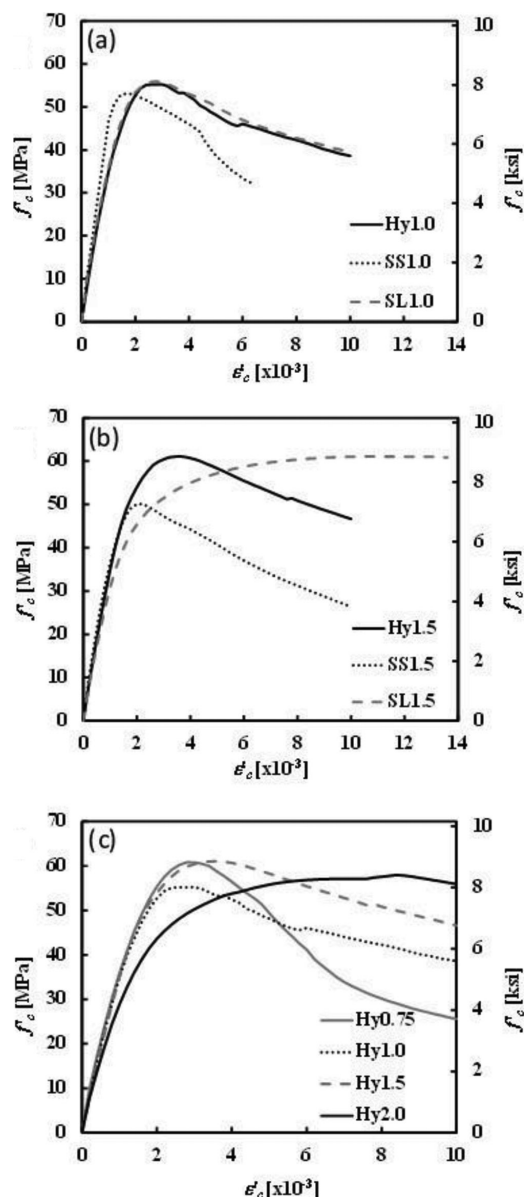
Fig. 4—Effect of hybridization on compression: (a) V_f = 1.0%; (b) V_f = 1.5%; and (c) hybrid mixtures variable V_f.

Fig. 5—Correlation of cylinder compressive strength ($f_{ck,100}$) over cube compressive strength ($f_{cc,150}$).

than expected and approximately equal to those of the cubes. Typically, with plain concrete, the strength measure obtained from cylinders is in the range of 80 to 85% of that from cubes[31]; end confinement effects are a probable underlying reason for the disparity, with the effects being more pronounced in cubes because of their lower aspect ratio. Steel fibers, in moderate percentages, do not significantly affect the maximum compressive strength. Therefore, the authors believe that confinement provided by the fibers in the horizontal direction partially negated the end-effect advantage enjoyed by the cubes, and thus drew the correlation factor closer to unity.

In the last 25 years, there has been a series of research efforts examining the effect of different specimen shapes and sizes on the compressive strength of concrete. Cylinders and cubes of various sizes have been tested by researchers to identify appropriate correlation factors. Gonnermann,[32] Day,[33] Mansur and Islam,[34] Mindess and Young,[35] and Neville[31] 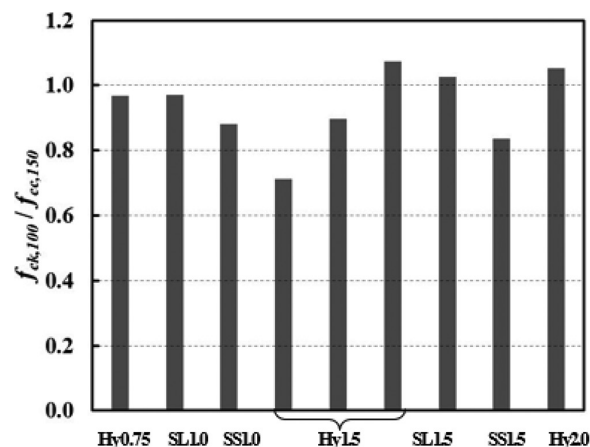are only few of those who compiled large databases of specimens for plain concrete, and more recently, Graybeal and Davis.[36] and Aslani[37] for concrete containing fibers. The outcome was that strength expressed by smaller specimens is expected to be somewhat higher relative to larger size specimens. This has been assumed to be due to larger size specimens having a greater likelihood of containing elements of low strength.[31] However, differences decrease with increasing compressive strengths.[31,35] This may constitute one more reason, apart for the confinement effect, to explain the correlation factor in compression obtained in this study.

Direct tension test results

The results obtained by the dog-bone specimens are presented in Table 4. The peak tensile strength f_t' was approximately the same for all batches with a mean value of 4.3 MPa (0.62 ksi) and a coefficient of variation of 12%. The variable f_t', normalized over the square root of the cylinder compressive strength, correlates well with the factor of 0.4 to 0.6, in MPa (0.07 to 0.09, in ksi), typical for plain concrete. Several cavities were noticed after testing in the specimen that contained 2.0% fibers per unit volume; for this reason, the peak load and the stiffness in Table 4, and the complete stress-strain curve, appear lower compared to the other tests in Fig. 6(c).

Figures 6(a) and 6(b) provide the stress-strain curve for the hybrid specimens versus the monofiber counterparts for V_f equal to 1.0% and 1.5%, respectively. The peak tensile strength is approximately the same for all specimens and is equal to the tensile strength of the matrix. After the peak stress is reached, the behavior is followed by a softening branch, particularly steep for the SS specimens because the short fibers are ineffective at relatively large crack widths. On the other hand, the Hy and SL specimens exhibit almost the same load resistance for the same strain in the post-cracking branch, despite the fact that HySFRC specimens contained only half of the long fibers of the SL specimens. Synergy for the HySFRC in direct tension is identified both in the elastic range by limited enhancement of the stiffness and in the post-peak regime by improved pullout strength of the long fibers. As expected, higher total fiber ratio results in higher post-cracking strength for the hybrid specimens, as shown in Fig. 6(c), except for Hy2.0, which was affected by casting difficulties as previously discussed.

Table 4—Direct tension test results

	Hy0.75	Hy1.0		SL1.0	SS1.0	Hy1.5			SL1.5	SS1.5	Hy2.0
Batch No.		1	2			1	2	3			
f_t', MPa (ksi)	4.78 (0.69)	3.74 (0.54)	4.93 (0.72)	3.99 (0.58)	4.69 (0.68)	4.63 (0.67)	3.79 (0.55)	3.39 (0.49)	4.34 (0.63)	4.77 (0.69)	3.91 (0.57)
CoV, %	5.9	6.1	2.3	7.2	5.0	—	4.1	10.1	4.1	6.2	—
Mean f_t', MPa (ksi)	4.78 (0.69)	4.33 (0.63)		3.99 (0.58)	4.69 (0.68)	3.94 (0.57)			4.34 (0.63)	4.77 (0.69)	3.91 (0.57)
$f_t'/\sqrt{f_{ck,100}'}$	0.61	0.57		0.53	0.64	0.49			0.56	0.67	0.51
ε_t', $\times 10^{-3}$	0.33	0.25	0.46	0.47	0.24	0.15	0.17	0.39	0.24	0.52	0.55
CoV, %	14.9	45.7	12.3	18.0	33.0	—	20.3	83.4	21.6	15.3	—
Mean ε_t', $\times 10^{-3}$	0.33	0.36		0.47	0.24	0.23			0.24	0.52	0.55
E_{ct}, GPa (ksi)	33.9 (4922)	45.0 (6537)	36.0 (5229)	36.5 (5308)	34.9 (5073)	49.7 (7215)	39.4 (5716)	38.4 (5580)	37.3 (5416)	32.9 (4773)	28.8 (4183)
CoV, %	6.1	50.8	1.5	24.3	12.7	—	15.2	10.2	12.7	8.5	—
Mean E_{ct}, GPa (ksi)	33.9 (4922)	40.5 (5883)		36.5 (5308)	34.9 (5073)	42.5 (6170)			37.3 (5416)	32.9 (4773)	28.8 (4183)
G, kJ/m² (ft·lb/ft²)	24.65 (514)	29.13 (608)		27.69 (578)	20.78 (433)	35.06 (732)			34.47 (719)	21.20 (442)	29.10 (607)

The behavior of FRC in tension appears to be somewhat nonlinear up to the point of the maximum load, possibly due in part to minor bending occurring in the uniaxial tension specimen. Thus, the E_{ct} value reported herein corresponds to secant stiffness at 40% f_t', consistent to the way it is calculated in the compression tests. Nevertheless, trends identified by the values for E_{ct} reported in Table 4 show that HySFRC is somewhat stiffer compared to the monofiber concrete with the same total amount of fibers. This is due to the microfibers stitching the microcracks.[12,38] In fact, the stiffness for the concrete with 1.0% hybrid fibers increased by 11% and 16% compared to the long fiber only and short fiber only specimens, respectively. The corresponding values for a total V_f equal to 1.5% were 14% and 29%. In Fig. 7, the modulus of elasticity normalized over the square root of the cylinder compressive strength shows these trends.

In an attempt to quantify the degree of synergy observed in the tension responses, the energy absorption capacity G was estimated as the area under the stress-strain curve up to 10 millistrain. The results are plotted against in Fig. 8 and reported numerically in Table 4. The energy absorption capacity for the concrete with 1.0% hybrid fibers increased by 5.2% and 40% compared to the long fiber only and short fiber only specimens, respectively. The corresponding values for a total V_f equal to 1.5% were 1.7% and 65%.

Modulus of rupture test results

Test results obtained by beams tested under four-point loading in accordance with ASTM C1609/C1609M-12[22] are presented in Table 5. Values include the stress at the onset of cracking (f_{cr}); the stress at the peak (f_p) and the corresponding deflection at the peak (δ_p); the stress at first crack (f_{cr}) normalized over the square root of the cylinder compressive strength $f_{ck,100}$; the toughness T_{150}^D; and the equivalent flexural strength ratio $R_{T,150}^D$. The stress at a point in the load-deflection curve was calculated using the corre-

sponding load measured at that point as $f_i = P_i \cdot L/(b \cdot d^2)$, where P_i is either the load at the onset of cracking (P_{cr}), as determined by experimental observation, or at the peak (P_p); L is the span length; and b and d are the average width and depth of the specimen, respectively. Toughness was calculated as the total area under the load-deflection curve up to a net deflection of $L/150$—that is, 3 mm (0.12 in.) in accordance with ASTM C1609/C1609M-12[22]

$$T_{150}^D = \int_0^\delta f(\delta)d\delta \tag{1}$$

The equivalent flexural strength ratio $R_{T,150}^D$ was obtained using the following equation

$$R_{T,150}^D = \frac{150 \cdot T_{150}^D}{f_{cr} \cdot b \cdot d^2} \cdot 100\% \tag{2}$$

The stress at the peak, f_p, did not coincide for any of the batches with the stress at first crack, f_{cr}, which occurred earlier in the load-deflection curves, and, therefore, the composite can be characterized as deflection hardening.[23] Figure 9 plots the f_{cr} normalized over the square root of the cylinder compressive strength $f_{ck,100}$ for all concrete batches. This value has been used as an indirect measure of the concrete tensile strength. Note that, for all specimens, the normalized flexural cracking strength is significantly higher than the corresponding typical value for plain concrete of approximately 0.6 to 0.7.[39]

Figure 10 plots the bending stress versus midspan deflection for the hybrid specimens versus the SL (long fibers only) and the SS (short fibres only) specimens for increasing fibers ratios. The hybrid composites are stronger in terms of ultimate load, have higher post-cracking stiffness, and possess higher fracture toughness. These observations are consis-
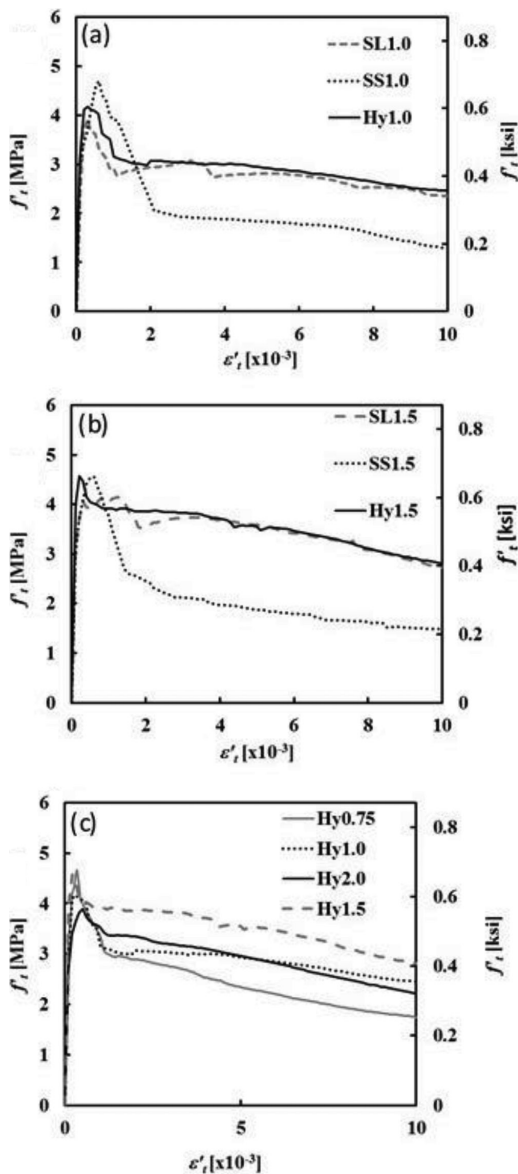
Fig. 6—Effect of hybridization on tensile response: (a) V$_f$ = 1.0%; (b) V$_f$ = 1.5%; and (c) hybrid mixtures variable V$_f$.

Fig. 7—Effect of hybridization on modulus of elasticity obtained by direct tension tests.
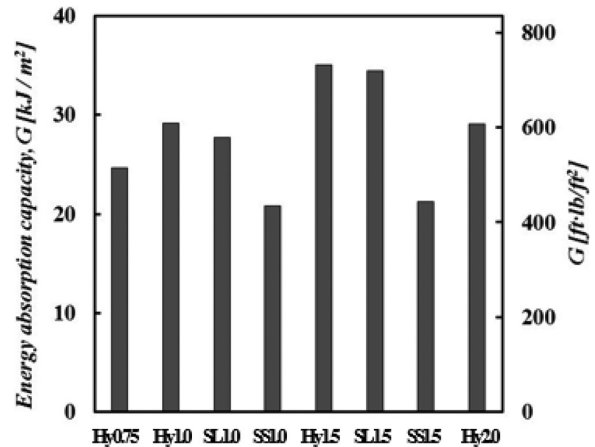
Fig. 8—Effect of hybridization on fracture energy in direct tension tests.

tent with experimental findings by Blunt and Ostertag.[40] Peak bending stress, post-cracking stiffness, and toughness increase for increasing fiber ratio as well as for the hybrid fiber specimens versus the monofiber counterparts.

Overall, the maximum bending stress was enhanced by 8% and 36% for the Hy1.0 against the SL1.0 and the SS1.0, respectively, while for a total volumetric ratio of fibers of 1.5%, the enhancement ratio was 9% and 52%, respectively. The corresponding values for toughness were 4% for Hy1.0 versus SL1.0, and 7% and 95% for Hy1.5 versus SL1.5 and SS1.5. It may be noted that these values are likely conservative estimates of the enhancement of properties because the hybrid mixtures were compared against mixtures with double the amount of long fibers or short fibers, respectively.

SUMMARY AND CONCLUSIONS

This paper investigates the influence of fiber hybridization on the mechanical response of normal-strength fiber-reinforced concrete. Tests under compression, direct tension, and four-
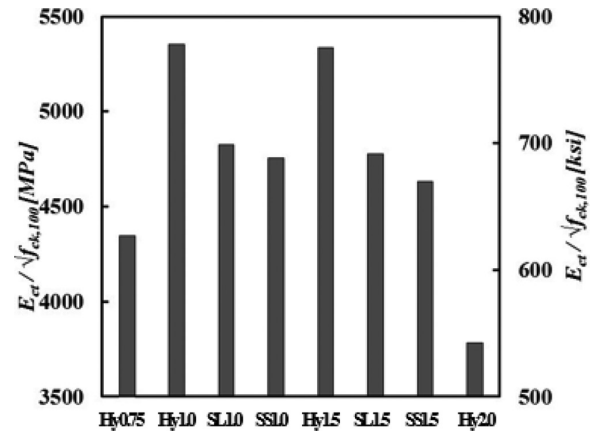
point bending were performed both with concrete containing hybrid fibers in a ratio of 1:1 as well as their corresponding counterparts containing a single type of fiber only in the same total volumetric ratio. Based on the results of the experimental investigation, the following observations can be made:

1. The peak compressive strength is not affected by fiber hybridization but the compressive strain capacity is. Hybridization, and especially the presence of short microfibers, has a large impact on the compressive stress-strain curve in a manner resembling a confinement effect. The strain at peak compressive strength, initial stiffness, and post-peak toughness are all beneficially influenced and should be taken into account in the analysis and design of members containing hybrid fibers.

2. The compressive strengths obtained from 100 mm (4 in.) diameter cylinders are closer to those obtained from 150 mm (6 in.) cubes than is normally seen with plain concrete. Confinement provided by the fibers may be partially negating the relatively stronger end confinement effects prevalent with cubes.

3. In direct tension, post-peak strength and fracture energy are enhanced with fiber hybridization. The synergy between fibers is increased at higher total fiber ratios.

4. Peak bending stress and fracture toughness increase due to enhanced pullout resistance of the longer fibers.

5. A novel dog-bone specimen configuration for tests in direct tension was developed and tested in this work. The

Table 5—Bending test results

|	Hy0.75	Hy1.0		SL1.0	SS1.0	Hy1.5			SL1.5	SS1.5	Hy2.0
Batch No.		1	2			1	2	3			
Mean f_{cr}, MPa (ksi)	6.64 (0.96)	8.39 (1.22)		7.68 (1.11)	6.35 (0.92)	9.47 (1.37)			8.28 (1.20)	6.66 (0.97)	11.06 (1.60)
Mean f_p, MPa (ksi)	6.956 (1.01)	9.75 (1.41)		9.05 (1.31)	7.15 (1.04)	10.98 (1.59)			10.12 (1.47)	6.68 (0.97)	11.71 (1.70)
$f_{cr}/\sqrt{f_{ck,100}}$	0.85	1.11		1.01	0.86	1.19			1.06	0.94	1.45
Mean δ_p, mm (in.)	0.35 (0.0138)	0.70 (0.0276)		0.84 (0.0331)	*	0.58 (0.0228)			0.65 (0.0256)	0.16 (0.0063)	0.85 (0.0335)
T^D_{150}, J (in.-lbf)	125 (1106)	155 (1372)		150 (1336)	—	168 (1486)			158 (1398)	86 (761)	217 (1920)
$R^D_{T,150}$, %	75	68		69	—	69			71	54	77

*Values not measured.
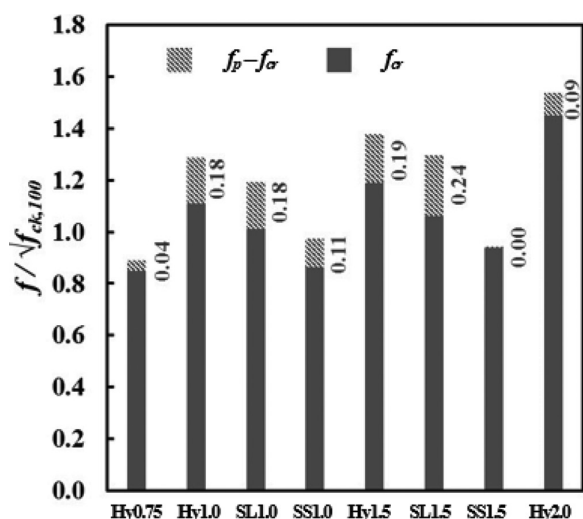
Fig. 9—Effect of hybridization on onset of cracking and peak bending stress.

new specimen configuration overcomes some deficiencies with previous configurations reported in literature, and it is easy to construct and test. It is suitable for concrete containing fibers. Test results show limited discrepancies and they are consistent with the current literature.

6. This study examines one combination of fibers and there were synergistic effects in stiffness, strength, and toughness. The extent to which synergistic effects occur with other combinations of fibers may vary.

7. In recognition of the gradual and multi-scale process of cracking, HySFRC has proven to be a promising, viable, and financially beneficial alternative to the single fiber-reinforced concrete.

AUTHOR BIOS

ACI member **Stamatina G. Chasioti** *is a PhD Candidate at the University of Toronto, Toronto, ON, Canada. She received her bachelor's and master's degrees from Democritus University of Thrace, Komotini, Greece. Her research interests include analysis and modeling of concrete structures using novel materials, reinforced concrete mechanics, and constitutive modeling.*

Frank J. Vecchio, *FACI, is a Professor in the Department of Civil Engineering at the University of Toronto. He is a member of Joint ACI-ASCE Committees 441, Reinforced Concrete Columns, and 447, Finite Element Analysis of Reinforced Concrete Structures. His research interests include nonlinear analysis and design of reinforced concrete structures, constitutive modeling, performance assessment and forensic investigation, and repair and rehabilitation of structures.*
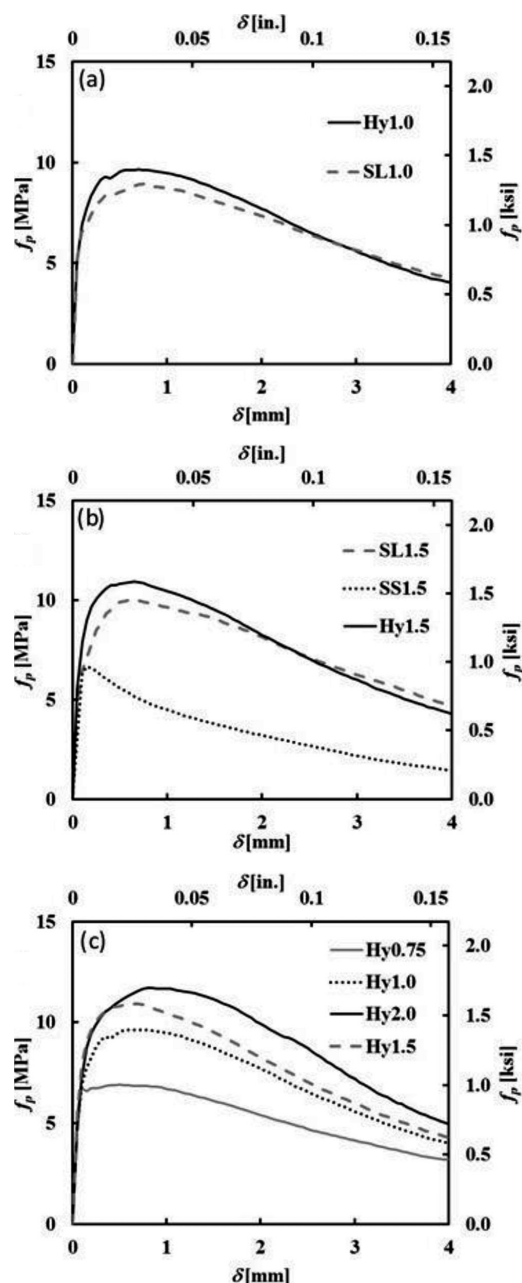
Fig. 10—Effect of hybridization on bending: (a) $V_f = 1.0\%$; (b) $V_f = 1.5\%$; and (c) hybrid mixtures variable V_f.

NOTATION

AR_f	=	fiber aspect ratio
CoV	=	coefficient of variation
d_f	=	fiber diameter
E_{cs}	=	secant modulus of elasticity obtained from compression tests
E_{ct}	=	secant modulus of elasticity obtained from tensile tests
E_f	=	fiber modulus of elasticity
$f_{cc,150}$	=	compressive strength of concrete obtained from cubes
$f_{ck,100}$	=	compressive strength of concrete obtained from cylinders
f_{cr}	=	bending stress at onset of cracking
f_p	=	peak bending stress
f_t'	=	peak tensile strength
f_{uf}	=	fiber ultimate tensile strength
l_f	=	fiber length
G	=	energy absorption capacity in direct tension
$R^D_{T,150}$	=	equivalent flexural strength ratio
T^D_{150}	=	toughness up to net deflection of $L/150$ of clear span length
V_f	=	total fiber volumetric ratio (w/w)
γ	=	measured unit weight of concrete
γ_n	=	nominal unit weight of concrete (calculated from composition)
ε_c'	=	strain at peak compressive stress
ε_t'	=	strain at peak tensile stress

REFERENCES

1. Balaguru, P. N., and Shah, S. P., *Fiber Reinforced Cement Composites*, McGraw Hill, New York, 1992.

2. Fischer, G., and Li, V. C., "Effect of Fiber Reinforcement on the Response of Structural Members," *Engineering Fracture Mechanics*, V. 74, No. 1-2, 2007, pp. 258-272. doi: 10.1016/j.engfracmech.2006.01.027

3. Banthia, N., and Sappakittipakorn, M., "Toughness Enhancement in Steel Fiber Reinforced Concrete Through Fiber Hybridisation," *Cement and Concrete Research*, V. 37, No. 9, 2007, pp. 1366-1372. doi: 10.1016/j.cemconres.2007.05.005

4. Bentur, A., and Mindess, S., *Fiber Reinforced Cementitious Composites*, Elsevier Applied Science, London, 1990.

5. Xu, G.; Magnani, S.; and Hannant, D. J., "Durability of Hybrid Polypropylene-Glass Fiber Cement Corrugated Sheets," *Cement and Concrete Composites*, V. 20, No. 1, 1998, pp. 79-84. doi: 10.1016/S0958-9465(97)00075-9

6. Shah, S. P., "Do Fibers Increase the Tensile Strength of Cement-Based Matrices," *ACI Materials Journal*, V. 88, No. 6, Nov.-Dec. 1991, pp. 595-602.

7. Lawler, J. S.; Zampini, D.; and Shah, S. P., "Microfiber and Macrofiber Hybrid Fiber-Reinforced Concrete," *Journal of Materials in Civil Engineering*, ASCE, V. 17, No. 5, 2005, pp. 595-604. doi: 10.1061/(ASCE)0899-1561(2005)17:5(595)

8. Wang, D. Z., "Analysis of Ultra-High Performance Fiber Reinforced Concrete Structures Using Truss Models," MASc thesis, Department of Civil Engineering, University of Toronto, Toronto, ON, Canada, 2014.

9. Chasioti, S. G., and Vecchio, F. J., "Hybrid Steel Fiber Reinforced Concrete Panels in Shear: Experimental Investigation," *Proceedings of HPFRCC7*, Stuttgart, Germany, 2015.

10. Plizzari, G. A.; Cangiano, S.; and Cere, N., "Postpeak Behavior of Fiber-Reinforced Concrete Under Cyclic Tensile Loads," *ACI Materials Journal*, V. 97, No. 2, Mar.-Apr. 2000, pp. 182-192.

11. Markovic, I.; Walraven, J. C.; and van Mier, J. G. M., "Experimental Evaluation of Fibre Pullout from Plain and Fibre Reinforced Concrete," *Proceedings of HPFRCC4*, Ann Arbor, MI, 2003.

12. Banthia, N., "A Study of Some Factors Affecting the Fiber-Matrix Bond in Steel Fiber Reinforced Concrete," *Canadian Journal of Civil Engineering*, V. 17, No. 4, 1990, pp. 610-620. doi: 10.1139/l90-069

13. Betterman, L. R.; Ouyang, C.; and Shah, S. P., "Fiber-Matrix Interaction in Microfiber-Reinforced Mortar," *Advanced Cement Based Materials*, V. 2, No. 2, 1995, pp. 53-61. doi: 10.1016/1065-7355(95)90025-X

14. Fantilli, A. P.; Mihashi, H.; and Nishiwaki, T., "Tailoring Hybrid Strain Hardening Cementitious Composites," *ACI Materials Journal*, V. 111, No. 2, Mar.-Apr. 2014, pp. 211-218. doi: 10.14359/51686563

15. Qian, C. X., and Stroeven, P., "Development of Hybrid Polypropylene-Steel Fibre-Reinforced Concrete," *Cement and Concrete Research*, V. 30, No. 1, 2000, pp. 63-69. doi: 10.1016/S0008-8846(99)00202-1

16. Banthia, N., and Soleimani, S. M., "Flexural Response of Hybrid Fiber-Reinforced Cementitious Composites," *ACI Materials Journal*, V. 102, No. 6, Nov.-Dec. 2005, pp. 382-389.

17. Pereira, E. B.; Fischer, G.; and Barros, J. A. O., "Effect of Hybrid Fiber Reinforcement on the Cracking Process in Fiber Reinforced Cementitious Composites," *Cement and Concrete Composites*, V. 34, No. 10, 2012, pp. 1114-1123. doi: 10.1016/j.cemconcomp.2012.08.004

18. Banthia, N.; Majdzadeh, F.; Wu, J.; and Bindiganavile, V., "Fiber Synergy in Hybrid Fiber Reinforced Concrete (HyFRC) In Flexure and Direct Shear," *Cement and Concrete Composites*, V. 48, 2014, pp. 91-97. doi: 10.1016/j.cemconcomp.2013.10.018

19. Chasioti, S. G., and Vecchio, F. J., "Shear Behavior and Crack Control Characteristics of Hybrid Steel Fiber Reinforced Concrete Panels," *ACI Structural Journal*, V. 114, No. 1, Jan.-Feb. 2017, pp. 209-220. doi: 10.14359/51689164

20. CSA A23.1-09/A23.2-09, "Concrete Materials and Methods of Concrete Construction/Test Methods and Standard Practices for Concrete," Canadian Standards Association, 2009, 674 pp.

21. ASTM C469/C469M, "Standard Test Method for Static Modulus of Elasticity and Poisson's Ratio of Concrete in Compression," ASTM International, West Conshohocken, PA, 2014, 5 pp.

22. ASTM C1609/C1609M-12, "Standard Test Methods for Flexural Performance of Fiber-Reinforced Concrete (Using Beam with Third-Point Loading)," ASTM International, West Conshohocken, PA, 2013, 9 pp.

23. Naaman, A. E., and Reinhardt, H. W., "Proposed Classification of HPFRC Composites Based on Their Tensile Response," *Materials and Structures*, V. 39, No. 5, 2007, pp. 547-555. doi: 10.1617/s11527-006-9103-2

24. Benson, S. D. P., and Karihaloo, B. L., "CARDIFRC—Development and Mechanical Properties. Part III: Uniaxial Tensile Response and Other Mechanical Properties," *Magazine of Concrete Research*, V. 57, No. 8, 2005, pp. 433-443. doi: 10.1680/macr.2005.57.8.433

25. Wille, K.; El-Tawil, S.; and Naaman, A. E., "Properties of Strain Hardening Ultra High Performance Fiber Reinforced Concrete (UHP-FRC) Under Direct Tensile Loading," *Cement and Concrete Composites*, V. 48, 2014, pp. 53-66. doi: 10.1016/j.cemconcomp.2013.12.015

26. Van Mier, J. G. M., *Fracture Processes of Concrete*, CRC Press, Boca Raton, FL, 1997.

27. Van Vliet, M. R. A., "Size Effect in Tensile Fracture of Concrete and Rock," PhD thesis, Delft University of Technology, Delft, the Netherlands, 2000.

28. Pantazopoulou, S. J., and Zanganeh, M., "Triaxial Tests of Fiber-Reinforced Concrete," *Journal of Materials in Civil Engineering*, ASCE, V. 13, No. 5, 2001, pp. 340-348. doi: 10.1061/(ASCE)0899-1561(2001)13:5(340)

29. Pantazopoulou, S. J., and Mills, R. H., "Microstructural Aspects of the Mechanical response of Plain Concrete," *ACI Materials Journal*, V. 92, No. 6, Nov.-Dec. 1995, pp. 602-616.

30. Rambo, D. A. S.; Silva, F. A.; and Filho, R. D. T., "Effect of Steel Fiber Hybridization on the Fracture Behavior of Self-Consolidating Concretes," *Cement and Concrete Composites*, V. 54, 2014, pp. 100-109. doi: 10.1016/j.cemconcomp.2014.02.004

31. Neville, A. M., *Properties of Concrete*, fourth and final edition, John Wiley & Sons, Inc., New York, 1996, pp. 581-594.

32. Gonnermann, H., "Effect of Size and Shape of Test Specimen on Compressive Strength of Concrete," *Proceedings of ASTM International*, V. 25, 1925, pp. 237-250.

33. Day, R., "Strength Measurement of Concrete Using Different Cylinder Sizes: A Statistical Analysis," *Cement, Concrete and Aggregates*, V. 16, No. 1, 1994, pp. 21-30. doi: 10.1520/CCA10557J

34. Mansur, M., and Islam, M., "Interpretation of Concrete Strength for Nonstandard Specimens," *Journal of Materials in Civil Engineering*, ASCE, V. 14, No. 2, 2002, pp. 151-155. doi: 10.1061/(ASCE)0899-1561(2002)14:2(151)

35. Mindess, S., and Young, J., *Concrete*, Prentice Hall, Englewood Cliffs, N.J., 1981.

36. Graybeal, B., and Davis, M., "Cylinder or Cube: Strength Testing of 80 to 200 MPa (11.6 to 29 ksi) Ultra-High-Performance Fiber-Reinforced Concrete," *ACI Materials Journal*, V. 105, No. 6, Nov.-Dec. 2008, pp. 603-609.

37. Aslani, F., "Effects of Specimen Size and Shape on Compressive and Tensile Strengths of Self-Compacting Concrete with or without Fibres," *Magazine of Concrete Research*, V. 65, No. 15, 2013, pp. 914-929. doi: 10.1680/macr.13.00016

38. Rossi, P.; Acker, P.; and Malier, Y., "Effect of Steel Fibres at Two Different Stages: The Material and The Structure," *Materials and Structures*, V. 20, No. 6, 1987, pp. 436-439. doi: 10.1007/BF02472494

39. Collins, M. P., and Mitchell, D., *Prestressed Concrete Structures*, Response Publications, Canada, 1997, pp. 57-120.

40. Blunt, J. D., and Ostertag, C. P., "Deflection Hardening and Workability of Hybrid Fiber Composites," *ACI Materials Journal*, V. 106, No. 3, May-June 2009, pp. 265-272.